ViReport v0.0.1

Niema Moshiri

2020-03-03

1 Input Dataset

The analysis was conducted on a dataset containing 188 sequences. The average sequence length was 29802.441489361703, with a standard deviation of 398.1848733754408. The earliest sample date was 2013-07-24, the median sample date was 2020-01-23, and the most recent sample date was 2020-02-28.

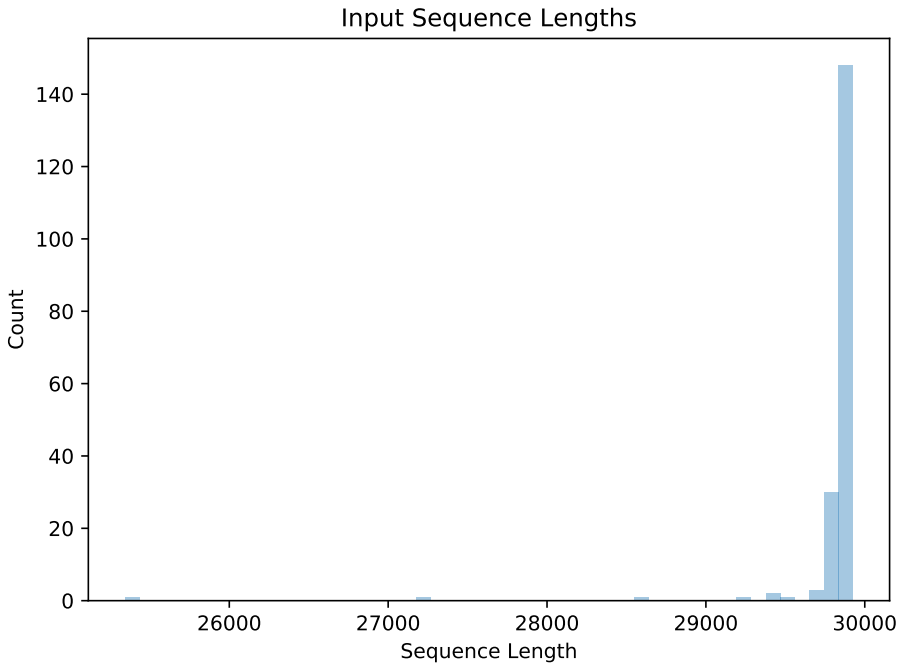

Figure 1: Distribution of input sequence lengths

2 Preprocessed Dataset

The input dataset was preprocessed such that sequences were given safe names: non-letters/digits in sequence IDs were converted to underscores. After preprocessing, the dataset contained 188 sequences. The average sequence length was 29802.441489361703, with a standard deviation of 398.1848733754408. The earliest sample date was 2013-07-24, the median sample date was 2020-01-23, and the most recent sample date was 2020-02-28.

3 Multiple Sequence Alignment

Multiple sequence alignment was performed using MAFFT (Katoh & Standley, 2013) in automatic mode. There were 30379 positions (16955 invariant) and 166 unique sequences in the multiple sequence alignment. Pairwise distances were computed from the multiple sequence alignment using the tn93 tool of HIV-TRACE (Pond et al., 2018). The average pairwise sequence distance was 0.00023931959492795083, with a standard deviation of 0.000241191693733296.

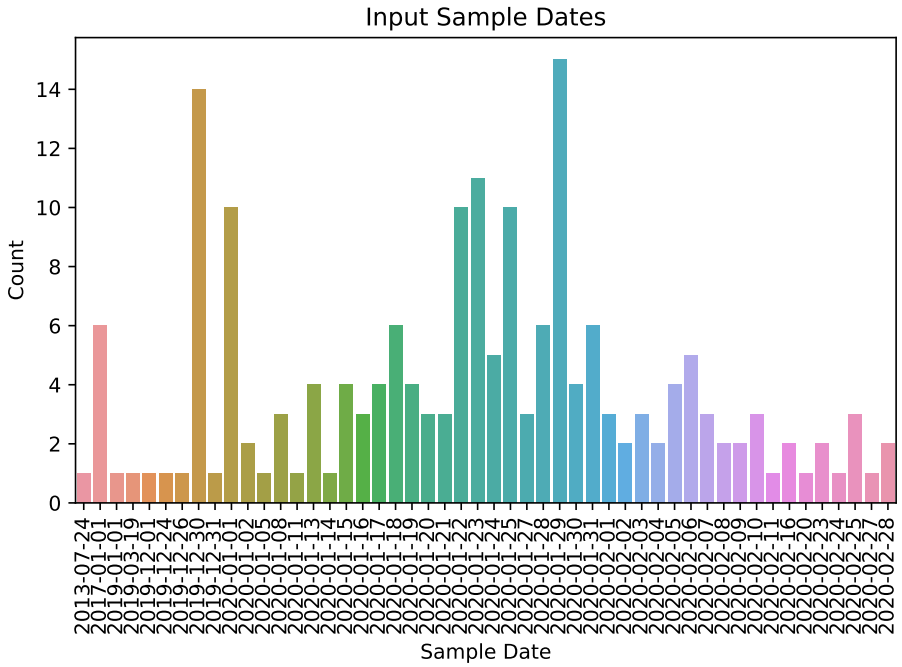

Figure 2: Distribution of input sample dates

4 Phylogenetic Inference

A maximum-likelihood phylogeny was inferred under the General Time-Reversible (GTR) model (Tavare, 1986) using FastTree 2 (Price et al., 2010) using a Gamma20-based likelihood. The inferred phylogeny was MinVar-rooted using FastRoot (Mai et al., 2017). Pairwise distances were computed from the phylogeny using TreeSwift (Moshiri, 2020). The maximum pairwise phylogenetic distance (i.e., tree diameter) was 0.003576486000000001, and the average pairwise phylogenetic distance was 0.0004088191522249731, with a standard deviation of 0.00040730380089063823.

5 Phylogenetic Dating

The rooted phylogeny was dated using treedater (Volz & Frost, 2017). The height of the dated tree was 0.2730446270571233 days, so given that the most recent sample was collected on 2020-02-28, the estimated time of the most recent common ancestor (tMRCA) was 2020-02-27.

6 Transmission Clustering

Transmission clustering was performed using TreeN93 (Moshiri, 2018) using pairwise phylogenetic distances. The total number of singletons (i.e., non-clustered individuals) was 111, and the total number of clusters (excluding singletons) was 21. The average cluster size (excluding singletons) was 3.1904761904761907, with a standard deviation of 1.3316315670580536, and the maximum and minimum cluster sizes were 6 and 2, respectively.

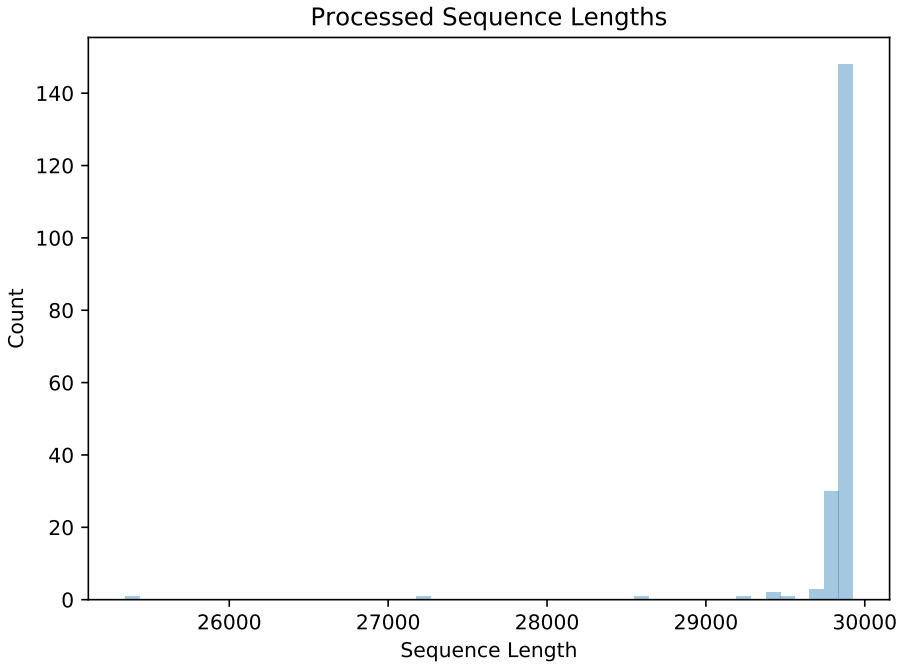

Figure 3: Distribution of preprocessed sequence lengths

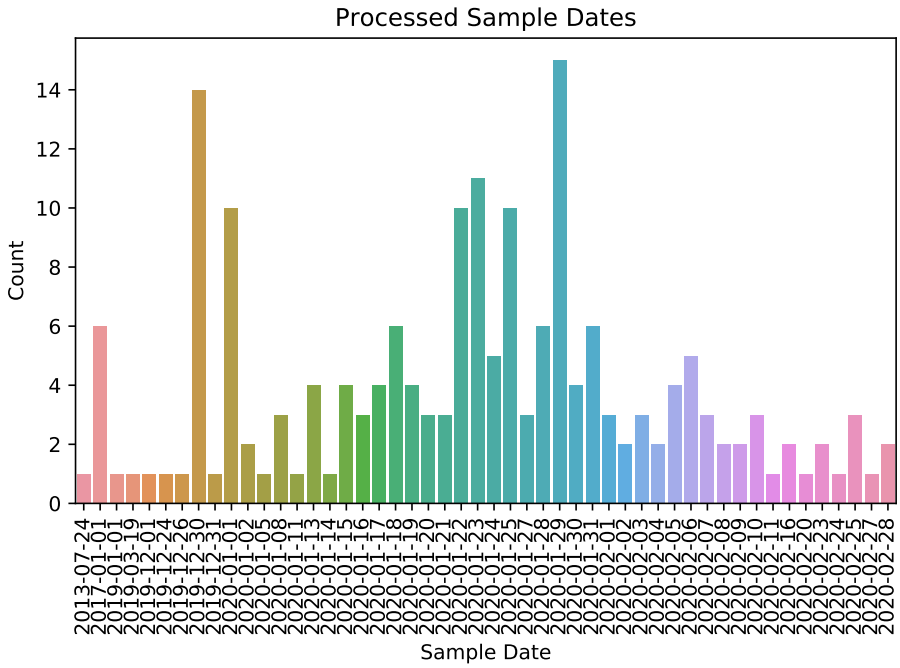

Figure 4: Distribution of preprocessed sample dates

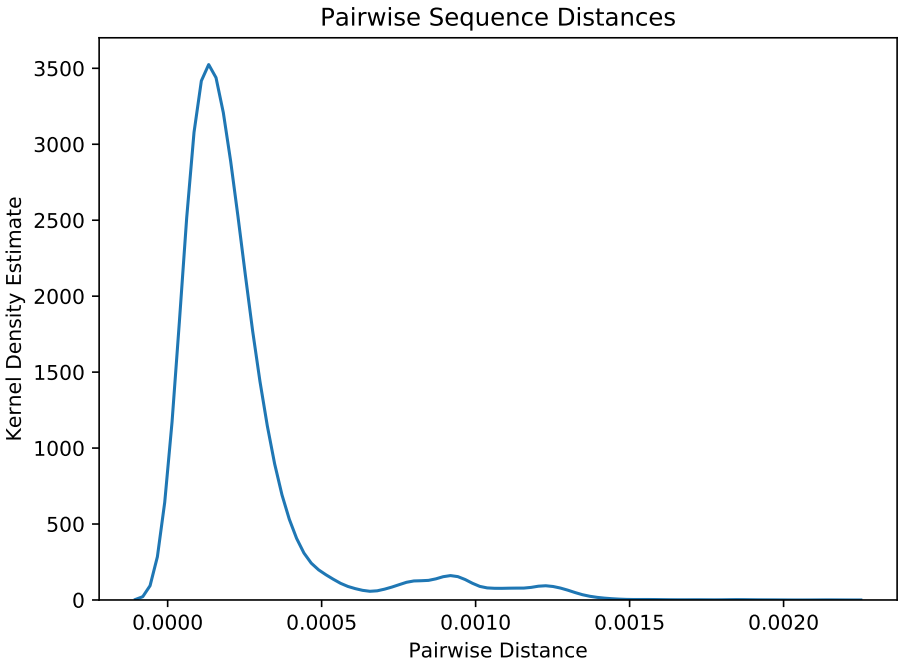

Figure 5: Distribution of pairwise sequence distances


BetaCoV_Nepal_61_2020_EPI_ISL_410301
BetaCoV_USA_IL1_2020_EPI_ISL_404253
BetaCoV_Guangdong_20SF014_2020_EPI_ISL_403934
BetaCoV_Shenzhen_SZTH_004_2020_EPI_ISL_406595
BetaCoV_Shenzhen_SZTH_003_2020_EPI_ISL_406594
BetaCoV_Foshan_20SF207_2020_EPI_ISL_406534
BetaCoV_USA_MA1_2020_EPI_ISL_409067
BetaCoV_Canada_ON_PHL2445_2020_EPI_ISL_413014
BetaCoV_Canada_ON_VIDO_01_2020_EPI_ISL_413015
BetaCoV_USA_CA3_2020_EPI_ISL_408008
BetaCoV_USA_CA4_2020_EPI_ISL_408009
BetaCov_Wuhan_WH02_2019_EPI_ISL_406799
BetaCoV_Singapore_3_2020_EPI_ISL_407988
BetaCoV_France_IDF0571_2020_EPI_ISL_411218
BetaCoV_France_IDF0515_2020_EPI_ISL_408430
BetaCoV_France_IDF0515_isl_2020_EPI_ISL_410984
BetaCoV_Chongqing_IVDC_CQ_001_2020_EPI_ISL_408481
BetaCoV_Shandong_IVDC_SD_001_2020_EPI_ISL_408482
_BetaCoV_Wuhan_HBCDC_HB_05_2020_EPI_ISL_412981
BetaCoV_Canada_BC_37_0_2_2020_EPI_ISL_412965
BetaCoV_Australia_NSW05_2020_EPI_ISL_412975
BetaCoV_Italy_SPL1_2020__EPI_ISL_412974
BetaCoV_Italy_INMI1_isl_2020_EPI_ISL_410545
BetaCoV_England_03_2020_EPI_ISL_412116
BetaCoV_Australia_VIC01_2020_EPI_ISL_406844
BetaCoV_South_Korea_KUMC02_2020_EPI_ISL_413018
BetaCoV_South_Korea_KUMC01_2020_EPI_ISL_413017
BetaCoV_South_Korea_SNU01_2020_EPI_ISL_411929
BetaCoV_Singapore_7_2020_EPI_ISL_410713
BetaCoV_Singapore_9_2020_EPI_ISL_410715
BetaCoV_Singapore_10_2020_EPI_ISL_410716
BetaCoV_Singapore_5_2020_EPI_ISL_410536
BetaCoV_Sweden_01_2020_EPI_ISL_411951
BetaCoV_USA_CA2_2020_EPI_ISL_406036
BetaCoV_France_IDF0386_2020_EPI_ISL_411220
BetaCoV_France_IDF0372_2020_EPI_ISL_410720
BetaCoV_France_IDF0386_2020_EPI_ISL_411219
BetaCoV_France_IDF0372_2020_EPI_ISL_406596
BetaCoV_France_IDF0373_2020_EPI_ISL_406597
BetaCoV_Taiwan_2_2020_EPI_ISL_406031
BetaCoV_Sydney_3_2020_EPI_ISL_408977
BetaCoV_Hong_Kong_VM20001988_2020_EPI_ISL_412029
BetaCoV_Singapore_8_2020_EPI_ISL_410714
BetaCoV_Wuhan_WH05_2020_EPI_ISL_408978
BetaCoV_Italy_INMI1_cs_2020_EPI_ISL_410546
BetaCov_Brazil_SPBR_02_2020_EPI_ISL_413016
BetaCoV_Japan_Hu_DP_Kng_19_027_2020_EPI_ISL_412969
BetaCoV_Hong_Kong_VB20026565_2020_EPI_ISL_412030
BetaCoV_Japan_Hu_DP_Kng_19_020_2020_EPI_ISL_412968
BetaCoV_Hefei_2_2020_EPI_ISL_412026
BetaCoV_Wuhan_Hu_1_2019_EPI_ISL_402125
BetaCoV_Germany_BavPat1_2020_EPI_ISL_406862
BetaCoV_Italy_CDG1_2020_EPI_ISL_412973
BetaCoV_Brazil_SPBR_01_2020_EPI_ISL_412964
BetaCoV_Finland_FIN_25_2020_EPI_ISL_412971
BetaCoV_Germany_Baden_Wuerttemberg_1_2020_EPI_ISL_412912
BetaCoV_Mexico_CDMX_InDRE_01_2020_EPI_ISL_412972
BetaCoV_Wuhan_IPBCAMS_WH_03_2019_EPI_ISL_403930
BetaCoV_Wuhan_IPBCAMS_WH_01_2019_EPI_ISL_402123
BetaCoV_Wuhan_IVDC_HB_04_2020_EPI_ISL_402120
BetaCoV_Henan_IVDC_HeN_002_2020_EPI_ISL_408487
BetaCoV_Wuhan_IVDC_HB_envF54_2020_EPI_ISL_408512
BetaCoV_Wuhan_IVDC_HB_envF13_2020_EPI_ISL_408511
BetaCoV_Wuhan_IPBCAMS_WH_02_2019_EPI_ISL_403931
BetaCoV_Taiwan_4_2020_EPI_ISL_411927
BetaCov_Taiwan_NTU02_2020_EPI_ISL_410218
BetaCoV_Wuhan_IPBCAMS_WH_04_2019_EPI_ISL_403929
BetaCoV_Wuhan_IVDC_HB_05_2019_EPI_ISL_402121
BetaCoV_Jiangsu_JS01_2020_EPI_ISL_411950
BetaCoV_Chongqing_ZX01_2020_EPI_ISL_408479
BetaCoV_Jiangsu_JS03_2020_EPI_ISL_411953
BetaCoV_Wuhan_IVDC_HB_01_2019_EPI_ISL_402119
BetaCoV_Wuhan_WIV04_2019_EPI_ISL_402124
BetaCoV_Jiangsu_JS02_2020_EPI_ISL_411952
BetaCoV_USA_CA5_2020_EPI_ISL_408010
BetaCoV_Guangdong_20SF174_2020_EPI_ISL_406531
BetaCoV_Guangdong_20SF028_2020_EPI_ISL_403936
BetaCoV_Guangdong_20SF040_2020_EPI_ISL_403937
BetaCoV_Sydney_2_2020_EPI_ISL_408976
BetaCoV_Wuhan_IVDC_HB_envF13_20_2020_EPI_ISL_408514
BetaCoV_Wuhan_IVDC_HB_envF13_21_2020_EPI_ISL_408515
BetaCoV_Singapore_2_2020_EPI_ISL_407987
BetaCoV_Singapore_6_2020_EPI_ISL_410537
BetaCoV_Guangdong_20SF201_2020_EPI_ISL_406538
BetaCoV_USA_CA8_2020_EPI_ISL_411955
_BetaCoV_Wuhan_HBCDC_HB_02_2019_EPI_ISL_412898
BetaCoV_Wuhan_WIV02_2019_EPI_ISL_402127
_BetaCoV_Wuhan_HBCDC_HB_04_2019_EPI_ISL_412900
BetaCoV_Jingzhou_HBCDC_HB_01_2020_EPI_ISL_412459
BetaCoV_Korea_KCDC12_2020_EPI_ISL_412872
BetaCoV_Zhejiang_WZ_01_2020_EPI_ISL_404227
BetaCoV_Jiangsu_IVDC_JS_001_2020_EPI_ISL_408488
BetaCoV_France_RA739_2020_EPI_ISL_410486
BetaCoV_Jiangxi_IVDC_JX_002_2020_EPI_ISL_408486
BetaCoV_Taiwan_CGMH_CGU_01_2020_EPI_ISL_411915
BetaCoV_Hangzhou_HZCDC0001_2020_EPI_ISL_407313
BetaCoV_Nonthaburi_61_2020_EPI_ISL_403962
_BetaCoV_Wuhan_HBCDC_HB_03_2019_EPI_ISL_412899
BetaCoV_Wuhan_WIV06_2019_EPI_ISL_402129

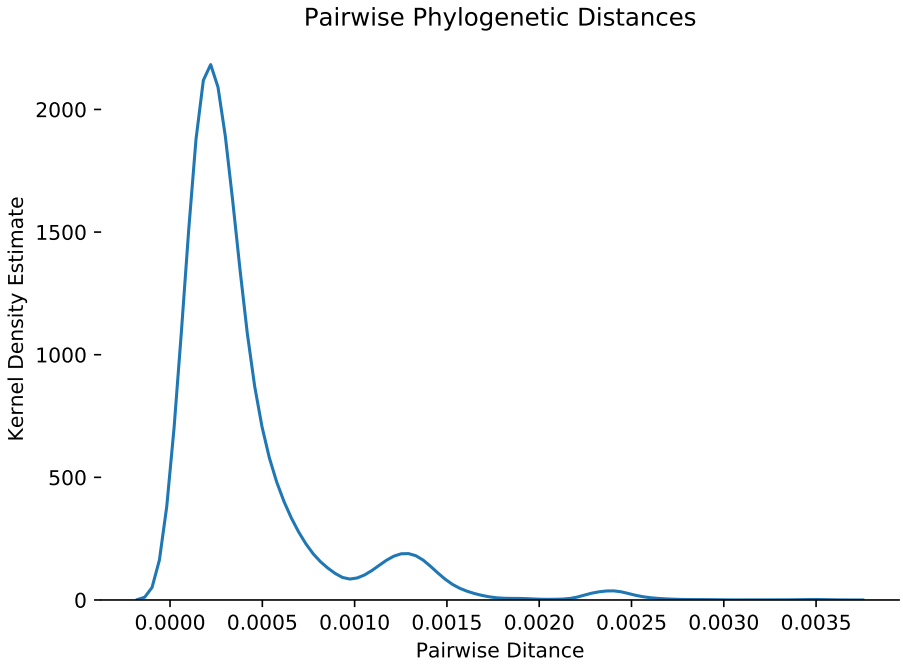

Figure 7: Distribution of pairwise phylogenetic distances

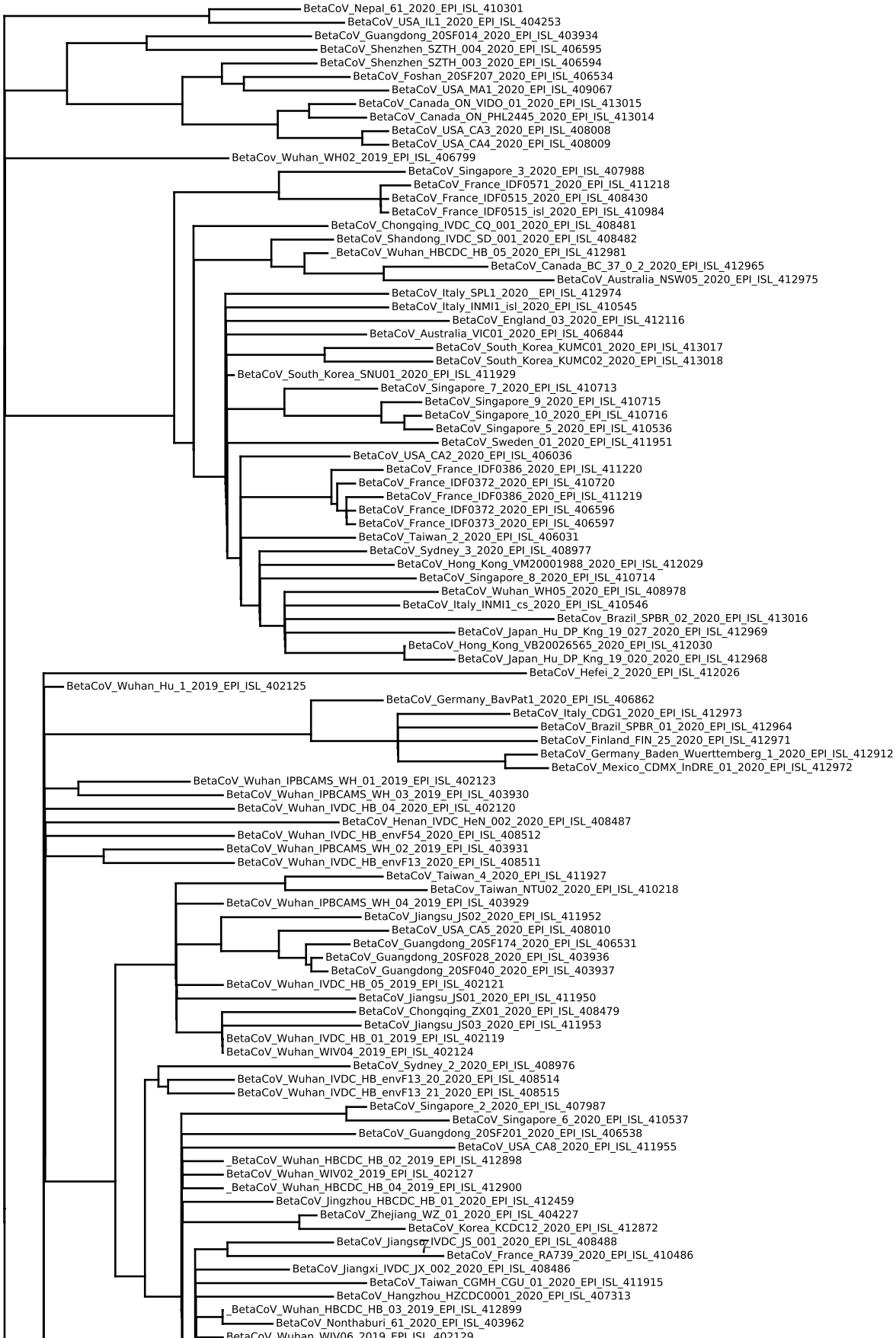
BetaCoV_Nepal_61_2020_EPI_ISL_410301
BetaCoV_USA_IL1_2020_EPI_ISL_404253
BetaCoV_Guangdong_20SF014_2020_EPI_ISL_403934
BetaCoV_Shenzhen_SZTH_004_2020_EPI_ISL_406595
BetaCoV_Shenzhen_SZTH_003_2020_EPI_ISL_406594
BetaCoV_Foshan_20SF207_2020_EPI_ISL_406534
BetaCoV_USA_MA1_2020_EPI_ISL_409067
BetaCoV_Canada_ON_VIDO_01_2020_EPI_ISL_413015
BetaCoV_Canada_ON_PHL2445_2020_EPI_ISL_413014
BetaCoV_USA_CA3_2020_EPI_ISL_408008
BetaCoV_USA_CA4_2020_EPI_ISL_408009
BetaCov_Wuhan_WH02_2019_EPI_ISL_406799
BetaCoV_Singapore_3_2020_EPI_ISL_407988
BetaCoV_France_IDF0571_2020_EPI_ISL_411218
BetaCoV_France_IDF0515_2020_EPI_ISL_408430
BetaCoV_France_IDF0515_isl_2020_EPI_ISL_410984
BetaCoV_Chongqing_IVDC_CQ_001_2020_EPI_ISL_408481
BetaCoV_Shandong_IVDC_SD_001_2020_EPI_ISL_408482
_BetaCoV_Wuhan_HBCDC_HB_05_2020_EPI_ISL_412981
BetaCoV_Canada_BC_37_0_2_2020_EPI_ISL_412965
BetaCoV_Australia_NSW05_2020_EPI_ISL_412975
BetaCoV_Italy_SPL1_2020__EPI_ISL_412974
BetaCoV_Italy_INMI1_isl_2020_EPI_ISL_410545
BetaCoV_England_03_2020_EPI_ISL_412116
BetaCoV_Australia_VIC01_2020_EPI_ISL_406844
BetaCoV_South_Korea_KUMC01_2020_EPI_ISL_413017
BetaCoV_South_Korea_KUMC02_2020_EPI_ISL_413018
BetaCoV_South_Korea_SNU01_2020_EPI_ISL_411929
BetaCoV_Singapore_7_2020_EPI_ISL_410713
BetaCoV_Singapore_9_2020_EPI_ISL_410715
BetaCoV_Singapore_10_2020_EPI_ISL_410716
BetaCoV_Singapore_5_2020_EPI_ISL_410536
BetaCoV_Sweden_01_2020_EPI_ISL_411951
BetaCoV_USA_CA2_2020_EPI_ISL_406036
BetaCoV_France_IDF0386_2020_EPI_ISL_411220
BetaCoV_France_IDF0372_2020_EPI_ISL_410720
BetaCoV_France_IDF0386_2020_EPI_ISL_411219
BetaCoV_France_IDF0372_2020_EPI_ISL_406596
BetaCoV_France_IDF0373_2020_EPI_ISL_406597
BetaCoV_Taiwan_2_2020_EPI_ISL_406031
BetaCoV_Sydney_3_2020_EPI_ISL_408977
BetaCoV_Hong_Kong_VM20001988_2020_EPI_ISL_412029
BetaCoV_Singapore_8_2020_EPI_ISL_410714
BetaCoV_Wuhan_WH05_2020_EPI_ISL_408978
BetaCoV_Italy_INMI1_cs_2020_EPI_ISL_410546
BetaCov_Brazil_SPBR_02_2020_EPI_ISL_413016
BetaCoV_Japan_Hu_DP_Kng_19_027_2020_EPI_ISL_412969
BetaCoV_Hong_Kong_VB20026565_2020_EPI_ISL_412030
BetaCoV_Japan_Hu_DP_Kng_19_020_2020_EPI_ISL_412968
BetaCoV_Hefei_2_2020_EPI_ISL_412026
BetaCoV_Wuhan_Hu_1_2019_EPI_ISL_402125
BetaCoV_Germany_BavPat1_2020_EPI_ISL_406862
BetaCoV_Italy_CDG1_2020_EPI_ISL_412973
BetaCoV_Brazil_SPBR_01_2020_EPI_ISL_412964
BetaCoV_Finland_FIN_25_2020_EPI_ISL_412971
BetaCoV_Germany_Baden_Wuerttemberg_1_2020_EPI_ISL_412912
BetaCoV_Mexico_CDMX_InDRE_01_2020_EPI_ISL_412972
BetaCoV_Wuhan_IPBCAMS_WH_01_2019_EPI_ISL_402123
BetaCoV_Wuhan_IPBCAMS_WH_03_2019_EPI_ISL_403930
BetaCoV_Wuhan_IVDC_HB_04_2020_EPI_ISL_402120
BetaCoV_Henan_IVDC_HeN_002_2020_EPI_ISL_408487
BetaCoV_Wuhan_IVDC_HB_envF54_2020_EPI_ISL_408512
BetaCoV_Wuhan_IPBCAMS_WH_02_2019_EPI_ISL_403931
BetaCoV_Wuhan_IVDC_HB_envF13_2020_EPI_ISL_408511
BetaCoV_Taiwan_4_2020_EPI_ISL_411927
BetaCov_Taiwan_NTU02_2020_EPI_ISL_410218
BetaCoV_Wuhan_IPBCAMS_WH_04_2019_EPI_ISL_403929
BetaCoV_Jiangsu_JS02_2020_EPI_ISL_411952
BetaCoV_USA_CA5_2020_EPI_ISL_408010
BetaCoV_Guangdong_20SF174_2020_EPI_ISL_406531
BetaCoV_Guangdong_20SF028_2020_EPI_ISL_403936
BetaCoV_Guangdong_20SF040_2020_EPI_ISL_403937
BetaCoV_Wuhan_IVDC_HB_05_2019_EPI_ISL_402121
BetaCoV_Jiangsu_JS01_2020_EPI_ISL_411950
BetaCoV_Chongqing_ZX01_2020_EPI_ISL_408479
BetaCoV_Jiangsu_JS03_2020_EPI_ISL_411953
BetaCoV_Wuhan_IVDC_HB_01_2019_EPI_ISL_402119
BetaCoV_Wuhan_WIV04_2019_EPI_ISL_402124
BetaCoV_Sydney_2_2020_EPI_ISL_408976
BetaCoV_Wuhan_IVDC_HB_envF13_20_2020_EPI_ISL_408514
BetaCoV_Wuhan_IVDC_HB_envF13_21_2020_EPI_ISL_408515
BetaCoV_Singapore_2_2020_EPI_ISL_407987
BetaCoV_Singapore_6_2020_EPI_ISL_410537
BetaCoV_Guangdong_20SF201_2020_EPI_ISL_406538
BetaCoV_USA_CA8_2020_EPI_ISL_411955
_BetaCoV_Wuhan_HBCDC_HB_02_2019_EPI_ISL_412898
BetaCoV_Wuhan_WIV02_2019_EPI_ISL_402127
_BetaCoV_Wuhan_HBCDC_HB_04_2019_EPI_ISL_412900
BetaCoV_Jingzhou_HBCDC_HB_01_2020_EPI_ISL_412459
BetaCoV_Zhejiang_WZ_01_2020_EPI_ISL_404227
BetaCoV_Korea_KCDC12_2020_EPI_ISL_412872
BetaCoV_Jiangsu_IVDC_JS_001_2020_EPI_ISL_408488
BetaCoV_France_RA739_2020_EPI_ISL_410486
BetaCoV_Jiangxi_IVDC_JX_002_2020_EPI_ISL_408486
BetaCoV_Taiwan_CGMH_CGU_01_2020_EPI_ISL_411915
BetaCoV_Hangzhou_HZCDC0001_2020_EPI_ISL_407313
_BetaCoV_Wuhan_HBCDC_HB_03_2019_EPI_ISL_412899
BetaCoV_Nonthaburi_61_2020_EPI_ISL_403962
BetaCoV_Wuhan_WIV06_2019_EPI_ISL_402129

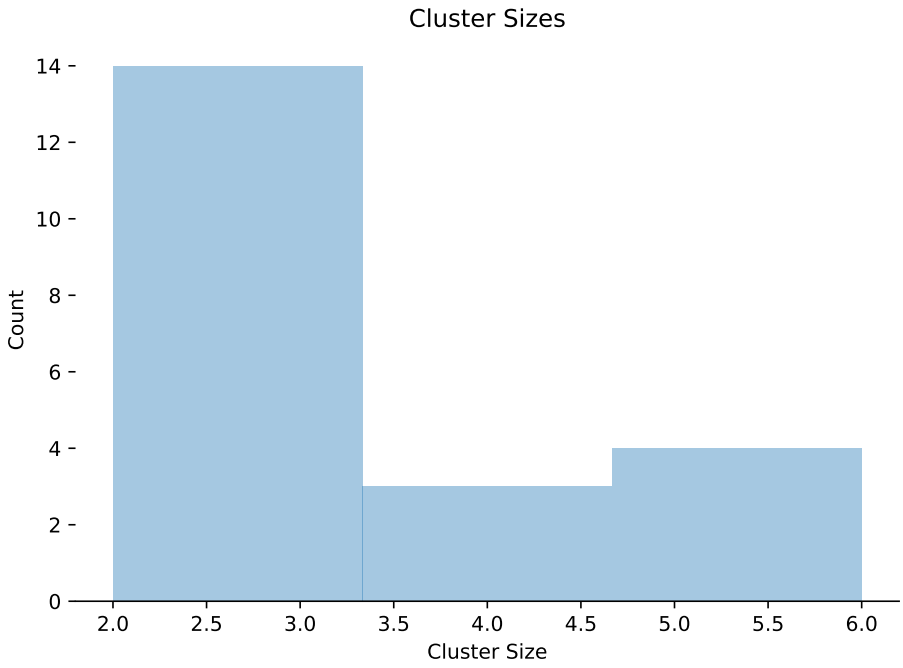

Figure 9: Distribution of cluster sizes (excluding singletons)